Nondeterministic gates for photonic single-rail quantum logic

A. P. Lund* and T. C. Ralph
Centre for Quantum Computer Technology, Department of Physics, University of Queensland, Queensland 4072, Australia
(Received 30 April 2002; published 16 September 2002)

We discuss techniques for producing, manipulating, and measuring qubits encoded optically as vacuum- and single-photon states. We show that a universal set of nondeterministic gates can be constructed using linear optics and photon counting. We investigate the efficacy of a test gate given realistic detector efficiencies.

DOI: 10.1103/PhysRevA.66.032307 PACS number(s): 03.67.Lx

I. INTRODUCTION

The standard method for encoding qubits in optics is to use the polarization degrees of freedom of single photons. This is sometimes referred to a dual-rail logic because it either does or does not use the occupation of two orthogonal polarization modes as the qubit [1]. This type of encoding is easy to manipulate at the single-qubit level and, recently, schemes for two-qubit operations have been introduced [2–4]. However, there is considerable fundamental interest in alternate encoding strategies.

One such strategy is single-rail logic [5]. Here, the qubit is defined by the occupation of a single optical mode. That is, the vacuum state, $|0\rangle$, represents the logical zero, while the single-photon state, $|1\rangle$, represents the logical one. Recently, experimental progress in creating superpositions of such states has been reported [6,7], and there has been a demonstration of entanglement swapping based on this logic [8].

In this paper we show how it is possible to construct a universal set of nondeterministic quantum gates for this encoding using only linear optics and detection. We investigate some simple experimental arrangements designed to test the performance of the gates, and conclude that demonstrations using state of the art technology are possible. It would presumably be possible to scale up these gates into near-deterministic gates using techniques similar to those proposed in Ref. [2], though we do not pursue this possibility here. Alternatively, the experiments proposed here may be viewed as stepping stones to multiphoton single-rail schemes, for which scalable architectures have been described [9].

A universal set of gates is formed by the control sign shift (CS) gate, the Hadamard gate, and the phase rotation gate. Nondeterministic CS gates for single-rail logic actually form the heart of identical gates for dual-rail logic [2,3]. We will borrow the most efficient and dedicated version of these, recently described by Knill [4], for this discussion. Phase rotations are easily implemented via phase delays, but the Hadamard gate presents a bigger challenge. Nevertheless, we show that a nondeterministic Hadamard gate can be implemented using only linear optics and detection.

The paper is arranged in the following way. In the next section we will review the construction of a CS gate. In Sec. III we will describe the construction of the Hadamard gate. In Sec. IV we will investigate the operation of our gates under nonideal conditions, and in Sec. V we will conclude.

II. CS GATE

We now review the operation of the linear optical network proposed by Knill [4] and shown in Fig. 1. The network is designed to be a nondeterministic CS gate with a probability of success of $\frac{2}{27}$.

In this gate the reflectivities of the beam splitters are $\eta_1 = \frac{1}{3}$ and $\eta_2 = \frac{1}{6}(3+\sqrt{6})$. Also, these beam splitters have a sign change on transmission for a beam incident on the black side. Therefore, the operator evolution through individual beam splitters looks like

$$a_{out} = \sqrt{\eta}\, a + \sqrt{1-\eta}\, b,$$

$$b_{out} = -\sqrt{1-\eta}\, a + \sqrt{\eta}\, b,$$

and the operator evolution through the entire gate with the above reflectivities is given by

$$a_{out} = \frac{1}{3}(-a + \sqrt{2}b + \sqrt{2}c - 2d), \tag{1}$$

$$b_{out} = \frac{1}{3}(-\sqrt{2}a - b + 2c + \sqrt{2}d), \tag{2}$$

$$c_{out} = \frac{1}{3\sqrt{2}}(\sqrt{3+\sqrt{6}}(\sqrt{2}a + c) + \sqrt{3-\sqrt{6}}(\sqrt{2}b + d)), \tag{3}$$

$$d_{out} = \frac{1}{3\sqrt{2}}(-\sqrt{3-\sqrt{6}}(\sqrt{2}a + c) + \sqrt{3+\sqrt{6}}(\sqrt{2}b + d)), \tag{4}$$

where the qubits enter into modes a and b, while modes c and d are prepared in single-photon Fock states. The input state to the gate can be written in a general way as

$$|\phi\rangle_{in} = c^\dagger d^\dagger(\alpha + \beta a^\dagger + \gamma b^\dagger + \delta a^\dagger b^\dagger)|0000\rangle. \tag{5}$$

The output state of the gate can be calculated by inverting the operator equations, Eqs. (1)–(4), thus obtaining the input

*Email address: lund@physics.uq.edu.au
Fax: +61 7 3365 1242.

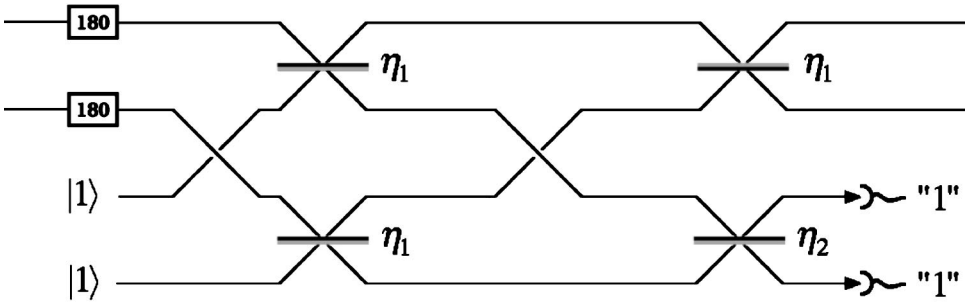

FIG. 1. Schematic of the CS gate proposed by Knill [4]. The beam splitters have a sign change upon transmission for light incident upon the black side. This sign convention is used for Eqs. (1)–(4). The reflectivities of the beam splitters are $\eta_1=\frac{1}{3}$ and $\eta_2=\frac{1}{6}(3+\sqrt{6})$.

operators in terms of the output operators, and substituting these for the operators appearing in Eq. (5). The form of the output state is quite long and hence will not be given here. However, if we condition our state by the simultaneous detection of a single photon in each of the lower two modes *c* and *d*, then the output state (unnormalized) is

$$|\phi\rangle_{out}=\sqrt{\frac{2}{27}}(\alpha+\beta a^{\dagger}_{out}+\gamma b^{\dagger}_{out}-\delta a^{\dagger}_{out}b^{\dagger}_{out})|0000\rangle. \tag{6}$$

This is control sign logic with a 180° sign flip. The probability of success is $\frac{2}{27}$, as predicted by Knill.

III. HADAMARD GATE

Superposition State Production. In order to create the single-rail Hadamard gate, a special superposition is used, and this resource must be generated. The state that is desired is the equal superposition state $|0\rangle+|1\rangle$. This state can be produced conditionally using only linear optics with coherent state and single-photon state inputs [10]. We consider a simpler, single-element approach similar to that employed in the experiment of Ref. [7]. This setup is shown in Fig. 2.

The parameter for the coherent state throughout will be given by the number χ. This parameter and the reflectivity of the beam splitter must be chosen so as to give the $|0\rangle+|1\rangle$ state with the higher-order terms giving very little contribution to the state. We must assume that χ is close to zero to satisfy this situation. The analysis of this system was performed using the expansion of the coherent state to the order of three photons. The coherent state $|\chi\rangle$ was written as (unnormalized)

$$|\chi\rangle\approx|0\rangle+\chi|1\rangle+\sqrt{\frac{1}{2}}\chi^2|2\rangle+\sqrt{\frac{1}{6}}\chi^3|3\rangle.$$

After the detection of one photon at the indicated output, the following reflectivity (η) is required for the coefficients of $|0\rangle$ and $|1\rangle$ to be equal at the other output:

$$\eta=\frac{-1+4\chi^2\pm\sqrt{1+8\chi^2}}{8\chi^2}. \tag{7}$$

The positive solution is used from here on in. Using this relationship, the value of χ required in order to make the coefficient of the second-order $|2\rangle$ term $100/\sqrt{2}$ times smaller (probability 5000 times smaller) is

$$\chi=-0.100\,74.$$

This means that the reflectivity must be

$$\eta=0.990\,244.$$

Using these values, however, the $|0\rangle+|1\rangle$ state is prepared only about 2% of the time. We can have better efficiency by allowing the second-order term to be larger. For example, choosing $\chi=-0.337\,14$ (corresponding reflectivity $\eta=0.919\,85$), the coefficient of the second-order $|2\rangle$ term is $10/\sqrt{2}$ times smaller (probability 50 times smaller), and now the state is prepared about 14% of the time.

Superposition Basis Measurements. Now that the superposition state $|0\rangle+|1\rangle$ has been produced, we also need to be able to measure in the basis state spanned by this and the orthogonal state $|0\rangle-|1\rangle$. The device that is used to perform measurements in this basis is a 50:50 beam splitter with a known, positive superposition state injected into one port and the unknown superposition injected into the other, as shown in Fig. 3.

One finds the state for a positive phase superposition to be

$$\frac{1}{2}|00\rangle+\sqrt{\frac{1}{2}}|10\rangle+\sqrt{\frac{1}{8}}(|20\rangle-|02\rangle)$$

and for a negative phase superposition to be

$$\frac{1}{2}|00\rangle+\sqrt{\frac{1}{2}}|01\rangle-\sqrt{\frac{1}{8}}(|20\rangle-|02\rangle).$$

If one photon is measured in the first mode then the unknown superposition had a positive phase, while one in the second mode indicates a negative phase superposition. The two su-

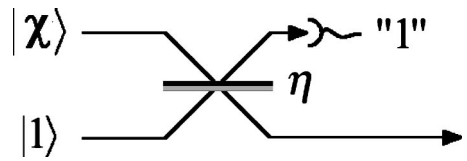

FIG. 2. Schematic of superposition production apparatus. $|\chi\rangle$ here is a coherent state with amplitude χ. The output (lower) mode of this device will contain a superposition $|0\rangle+|1\rangle$ with small higher-order terms after the correct detection event has occurred.

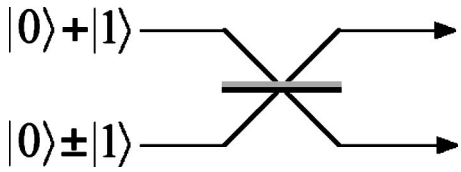

FIG. 3. Schematic for a device that performs measurements in the superposition basis $|0\rangle \pm |1\rangle$. The state to be measured is in the lower mode while the upper mode contains the state produced by the device described in Fig. 2. $|0\rangle + |1\rangle$ is detected with certainty when one and only one photon is measured in the top mode, and $|0\rangle - |1\rangle$ is detected when one photon is found only in the lower mode.

perpositions cannot be distinguished if zero total photons are counted in both modes or if two photons are measured in one mode. The measurement succeeds one half of the time.

Hadamard Gate. Now we have enough tools to perform the task that is desired. Figure 4 shows the construction of a single-rail Hadamard gate.

This gate requires two $|0\rangle + |1\rangle$ superpositions, one CS gate (as described in the preceding section), and one $|0\rangle \pm |1\rangle$ measurement. If the input is arbitrary (i.e., $\alpha|0\rangle + \beta|1\rangle$), then the bottom two modes at the far left can be described by the state

$$|\Phi\rangle = \alpha|00\rangle + \alpha|01\rangle + \beta|10\rangle + \beta|11\rangle,$$

where the first number is the number state of the upper mode. After the control sign operation, the state looks like

$$|\Phi\rangle = \alpha|00\rangle + \alpha|01\rangle + \beta|10\rangle - \beta|11\rangle.$$

Now a $|0\rangle \pm |1\rangle$ measurement is made on the top mode from the control sign gate. If we only take the positive result then the output state in the output mode is

$$|\psi\rangle = \alpha(|0\rangle + |1\rangle) + \beta(|0\rangle - |1\rangle),$$

which is Hadamard logic. Note that differential propagation produces a phase rotation

$$|\psi;t\rangle = e^{-i\omega\hat{a}^\dagger\hat{a}t}(|0\rangle + |1\rangle) = |0\rangle + e^{-i\omega t}|1\rangle.$$

This allows us to apply arbitrary rotations and thus completes our universal set of gates.

IV. TESTING THE GATES

In our discussion so far we have assumed unit detector efficiency and the ability to differentiate between zero, one,

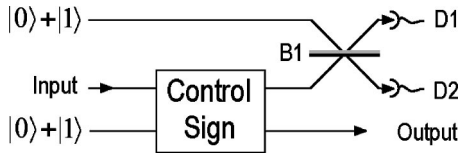

FIG. 4. Schematic of the Hadamard gate constructed using devices from Figs. 1, 2, and 3. The $|0\rangle + |1\rangle$ states are assumed to be created by a device similar to that in Fig. 2.

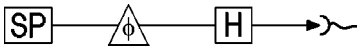

FIG. 5. Schematic of experimental test modeled to simulate the functionality of these gates using realistic detectors. SP denotes the $|0\rangle + |1\rangle$ production device (Fig. 2), ϕ performs a phase shift of the type $|0\rangle + e^{i\phi}|1\rangle$, and H denotes a Hadamard gate, as shown in Fig. 4.

and two photons. Off-the-shelf photon counters, on the other hand, have efficiencies of around 65% and can only differentiate between zero or more photons. This would be insufficient for demonstrating our single-rail gates. However, state of the art detectors have recently been described [11] with 90% efficiency and the ability to differentiate between zero, one, and two photons. We now model the performance of a simple single-rail test circuit if implemented with these state of the art detectors. The test circuit is shown in Fig. 5.

In the figure, SP produces the state $|0\rangle + |1\rangle$ nondeterministically, H is a Hadamard gate, ϕ is a phase shift, and there is a detector after the Hadamard gate. After the phase shift, the state looks like (unnormalized)

$$|\psi\rangle = |0\rangle + e^{i\phi}|1\rangle.$$

This state is passed through the Hadamard gate; as a result, the output state at the detector is (unnormalized)

$$|\psi\rangle = (1 + e^{i\phi})|0\rangle + (1 - e^{i\phi})|1\rangle.$$

As the phase shift ϕ is changed, the superposition at the output changes from $|0\rangle$ to $|1\rangle$ over the range of $\phi = 0$ to $\phi = \pi$, ideally with 100% visibility.

Photon loss in inefficient detectors is included in the analysis of the gate by modeling the inefficient detector as a beam splitter of transmittivity equivalent to the efficiency of the detector followed by a perfect detector. The reflected mode is traced over. Each of the detectors used in the construction of the Hadamard gate and the $|0\rangle + |1\rangle$ state production devices was simulated by this technique. Figure 6 shows the results of this simulation. The $|0\rangle + |1\rangle$ state producer (Fig. 2) uses a coherent strength of $\chi = -0.337\,14$ and,

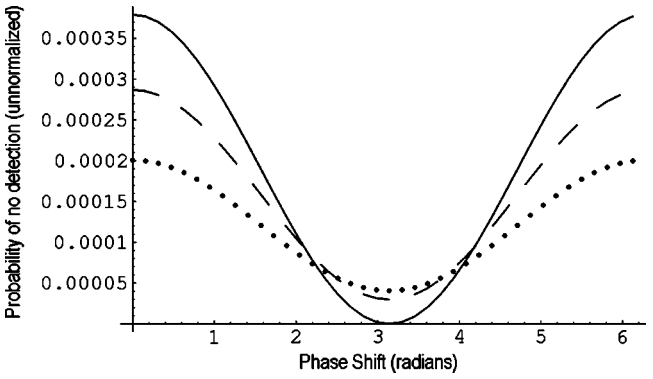

FIG. 6. Plot of detection probability vs the variation of the phase ϕ in Fig. 5. The solid line is a simulation with 100% efficient detectors, the dashed line with 90% efficient detectors, and the dotted line with 80% efficient detectors. The visibilities of these fringes are 1.00, 0.91, and 0.66, respectively.

by Eq. (7), a reflectivity of $\eta = 0.919\,85$. Shown is the probability of detecting zero photons in the output, given the correct combination of conditioning detector results. The probability is not normalized to this conditioning, so the y axis reflects the probability of obtaining this event (including the conditioning probability) for a single run. The x axis is the size of the phase shift taken relative to the phase of the coherent states, which produce the $|0\rangle + |1\rangle$ superposition states used both as inputs and as gate resources.

Figure 6 shows detectors of 100% efficiency (solid line), 90% efficiency (dashed line), and 80% efficiency (dotted line) using the photon loss model described above. The visibility of these curves is unity for 100%, 0.81 for 90%, and 0.66 for 80% efficient detectors.

From the results in Fig. 6 it is seen that for this arrangement of gates the probability of obtaining an output that has been successfully postselected is low, making a demonstration with current photon source technology extremely demanding. This occurs because a cascade of nondeterministic gates like this requires each gate to have successful postselection simultaneously. However, if quantum memory were available it would be possible to produce and store the superposition states "off-line." Then, in principle, the probability of gate success could be up to $\frac{1}{54}$.

V. CONCLUSION

We have shown that a universal set of gates can be implemented nondeterministically for the qubit encoding in which the vacuum state $|0\rangle$ represents logical zero and the single photon state $|1\rangle$ represents logical one. The implementation uses only linear optics and photodetection. It was also shown that a demonstration of the operation of these gates is plausible from the point of view of current detector technology.

ACKNOWLEDGMENTS

We acknowledge the support of the Australia Research Council and ARDA.

[1] G.J. Milburn, Phys. Rev. Lett. **62**, 2124 (1988).
[2] E. Knill, R. Laflamme, and G. Milburn, Nature (London) **409**, 46 (2001).
[3] T.C. Ralph, A.G. White, W.J. Munro, and G.J. Milburn, Phys. Rev. A **65**, 012314 (2001).
[4] E. Knill, e-print quant-ph/0110144.
[5] Hai-Woong Lee and Jaewan Kim, Phys. Rev. A **63**, 012305 (2001).
[6] K.J. Resch, J.S. Lundeen, and A.M. Steinberg, Phys. Rev. Lett. **88**, 113601 (2002).
[7] A.I. Lvovsky and J. Mlynek, e-print quant-ph/0202164.
[8] E. Lombardi, F. Sciarrino, S. Popescu, and F. De Martini, Phys. Rev. Lett. **88**, 070402 (2002).
[9] T.C. Ralph, W.J. Munro, and G.J. Milburn, e-print quant-ph/0110115.
[10] D.T. Pegg, L.S. Phillips, and S.M. Barnett, Phys. Rev. Lett. **81**, 1604 (1998).
[11] S. Takeuchi *et al.*, Appl. Phys. Lett. **74**, 1063 (1999); J. Kim *et al.*, *ibid.* **74**, 902 (1999).